Low-Melting-Point Titanium-Base Brazing Alloys—Part 2: Characteristics of Brazing Ti-21Ni-14Cu on Ti-6Al-4V Substrate

E. Chang and C.-H. Chen

Filler metal of a low-melting-point (917 °C) Ti-21Ni-14Cu was brazed onto the substrate of Ti-6Al-4V alloy at 960 °C for 2, 4, and 8 h to investigate the microstructural evolution and electrochemical characteristics of the brazed metal as a function of the period of brazing time. Optical microscopy, scanning and transmission electron microscopy, and x-ray diffractometry were used to characterize the microstructure and phase of the brazed metal; also, the potentiostat was used for corrosion study. Experimental results indicate that diffusion of copper and nickel from the filler metal into the equiaxed α plus intergranular β structure of Ti-6Al-4V substrate causes the lamellar Widmanstätten structure to form. The intermetallic Ti_2Ni phase existing in the prior filler metal diminishes, while the Ti_2Cu phase can be identified for the metal brazed at 960 °C for 2 h, but the latter phase decreases with time. Advantage might be taken from the evidence of faster diffusion of nickel than copper along the β phase to the substrate. In deaerated Hank's solution, corrosion potential, corrosion current density, and critical potential for active-to-passive transition decrease while the passivation range broadens with the period of brazing time. However, all the brazed metals, immersed for different periods in oxygen-saturated Hank's solution, show similar corrosion behavior, irrespective of the brazing time.

Keywords brazing, diffusion, electrochemical property, microstructure, titanium

1. Introduction

Titanium alloys joined by titanium-base brazing filler metals possess both excellent mechanical properties and good corrosion resistance (Ref 1, 2). In this area of study, attention has been paid to the development and application of lower-melting-point filler metals, with which brazing can be undertaken below the β transus or the α-β transformation temperature (Ref 3, 4). Also, it is known that brazing at lower temperature for titanium alloys can minimize the undesirable lamellar structure and grain growth at weld.

Recently, a titanium filler metal of the chemical composition Ti-21Ni-14Cu with a low melting point of 917 °C was studied for the microstructure, phase, and electrochemical property of the alloy, and it was found that the alloy exhibits the combined merit of low melting point and good corrosion resistance relative to the two-component Ti-28Ni and four-component Ti-35Zr-15Cu-15Ni or Ti-42.5Zr-10Cu-5Ni filler metals (Ref 5). However, as with other titanium fillers, brittle intermetallics such as Ti_2Ni and Ti_2Cu were still identified, and whether diffusion during brazing can substantially diminish these phases was considered, as well as how the change in chemical compositions after diffusion affects the electrochemical property of the Ti-21Ni-14Cu filler metal. In this work, the Ti-21Ni-14Cu filler metal was tested and brazed onto the Ti-6Al-4V substrate, and the changes in microstructure, phase, and the electrochemical behavior of the brazed metal in deaerated and oxygen-saturated Hank's solution were studied as a function of brazing time. Optical microscopy, transmission electron microscopy (TEM), and x-ray diffractometry (XRD) were used to characterize the microstructure and phase of the brazed metal, meanwhile the potentiostat was used for corrosion study.

E. Chang and **C.-H. Chen,** Department of Materials Science and Engineering, National Cheng-Kung University, Tainan 701, Taiwan.

2. Materials and Methods

Titanium-base filler metal of the composition Ti-21Ni-14Cu investigated in Ref 5 was chosen for brazing. To facilitate the specimen preparation, filler metal was directly melted onto the substrate of dimensions 40 × 40 × 3 mm with a central

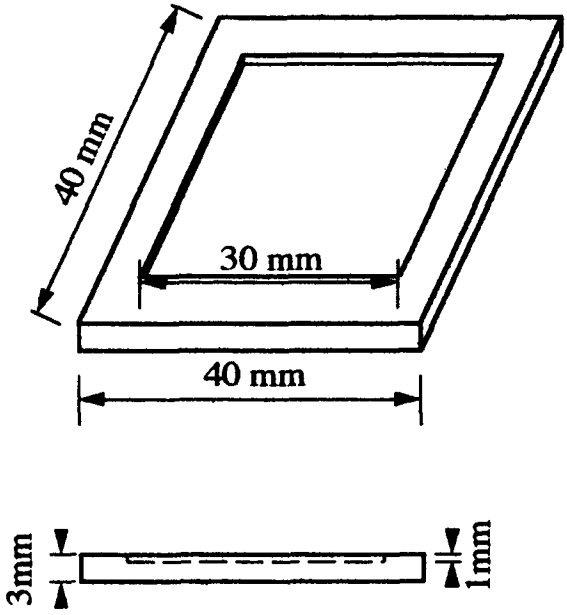

Fig. 1 Specimen for brazing Ti-21Ni-14Cu on Ti-6Al-4V substrate

sink of dimensions 30 × 30 × 1 mm as shown in Fig. 1. Ti-21Ni-14Cu metal powders of 0.4 g, evenly inserted into the sink, were preheated at 800 °C before melting and brazing at 960 °C for 2, 4, and 8 h under a vacuum of $<1 \times 10^{-5}$ torr, and after brazing the specimen was furnace cooled. Brazing time was varied in the investigation of the evolution of microstructure and corrosion behavior.

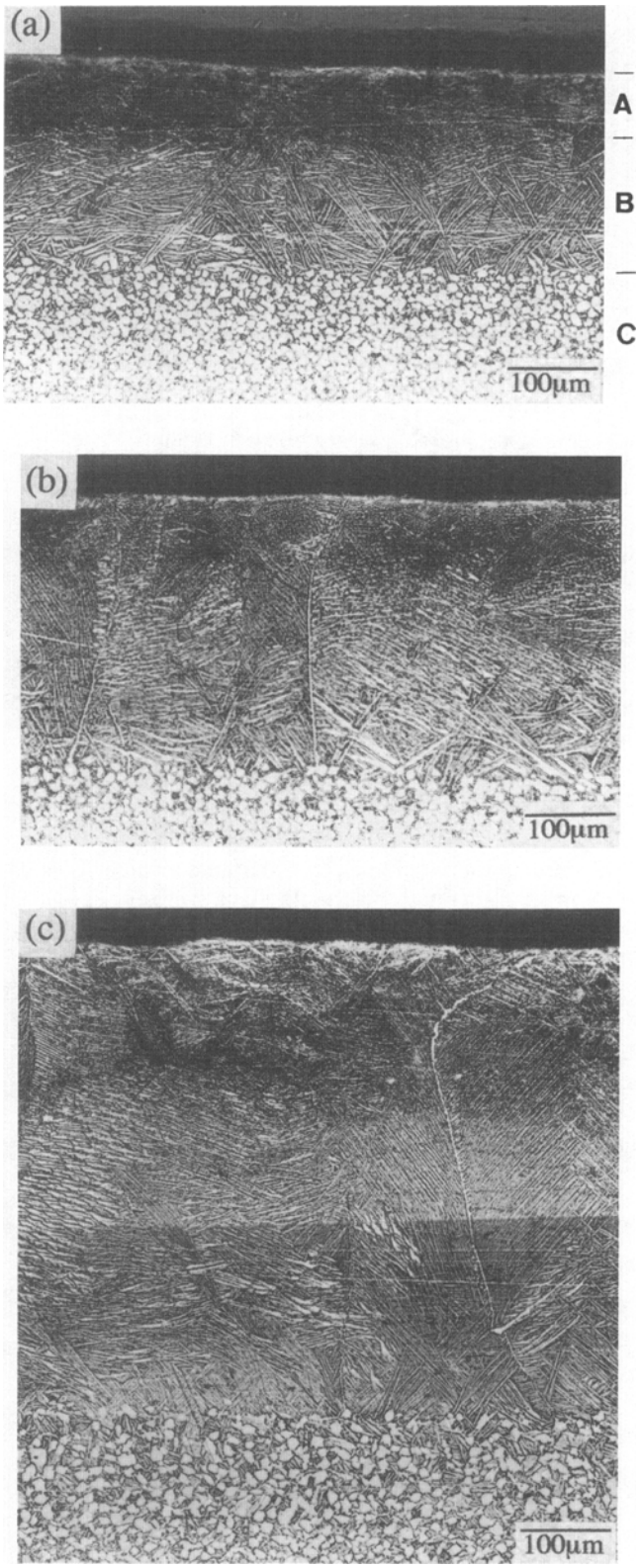

Fig. 2 Light optical micrography from cross section of (a) A2, (b) A4, and (c) A8 specimens brazed at 960 °C for 2, 4, and 8 h, respectively

Microstructural examinations were conducted by light optical microscopy (LOM) and TEM techniques. For LOM, the brazed specimens were ground, polished, and swab etched with Kroll's solution (3 mL HF, 36 mL HNO_3, 100 mL H_2O) for 15 s and then examined in a Nikon microscope (Nikon Corporation, Tokyo, Japan). For TEM observation, the specimens near the brazed surface were ground and thinned by jet electropolishing at 13 to 15 V and –40 to –50 °C, using 200 mL methanol + 115 mL 1-butanol + 20 mL 70% perchloric acid as solution. The thin foil was examined in the JEOL JEM200CX scanning TEM (JEOL Ltd., Tokyo, Japan). Phase identity from the surface of brazed specimens was done by XRD using the Rigaku D/Max III,V diffractometer (Rigaku Corporation, Tokyo, Japan) with Cu Kα radiation operated at 30 KV in voltage, 20 mA in current, and 4°/min in scan speed. JEOL JSM 840 Multi-function SEM/energy-dispersive x-ray (EDX) and JEOL JSM 35/WDS were employed for structural and elemental observations (JEOL Ltd., Tokyo, Japan).

For the present experiment, both the deaerated and aerated Hank's solutions were used for corrosion study. The specimens for study were taken from near the surface of the brazed metals, and the method of potentiodynamic polarization assessment of the brazed metals was similar to that described in Ref 5.

3. Results and Discussion

Optical micrographs of the brazed Ti-21Ni-14Cu on Ti-6Al-4V substrate at 960 °C for 2 (A2 specimen), 4 (A4 specimen), and 8 h (A8 specimen) are shown in Fig. 2. The cross-sectional microstructure after brazing for 2 h (Fig. 2a) consists of three zones. Zone A is the location of the original filler metal showing fine featureless structure at optical microscope level. Zone B is the interdiffusion zone; during brazing in this zone, diffusion of copper and nickel atoms from the liquid filler metal into the original equiaxed α plus intergranular β substrate has transformed the structure into β phase, which, on cooling, further transforms into lamellar α plus β Widmanstätten structure. The mechanism of mass transport during the isothermal diffusion brazing has been proposed (Ref 6). On cooling from β phase at high temperature, platelike α phase (light) nucleates at the grain boundary of β phase and grows along $[110]_\beta$ directions, leaving untransformed interplate β phase (dark) (Ref 7). The structure of Ti-6Al-4V substrate in zone C, consisting of equiaxed α (light) and intergranular β (dark), coarsens slightly during the brazing treatment. After brazing for 4 and 8 h as shown in Fig. 2(b) and (c), respectively, the structure becomes Widmanstätten zone B and equiaxed α plus intergranular β of the original Ti-6Al-4V substrate (zone C), while zone A disappears. The depth of brazing-affected zone (defined as zone A + zone B) is about 270 μm for A2 specimen; as the brazing time increases and inward diffusion of copper and nickel prevails, the depths increase to 320 and 580 μm accordingly after 4 and 8 h of brazing treatment, respectively.

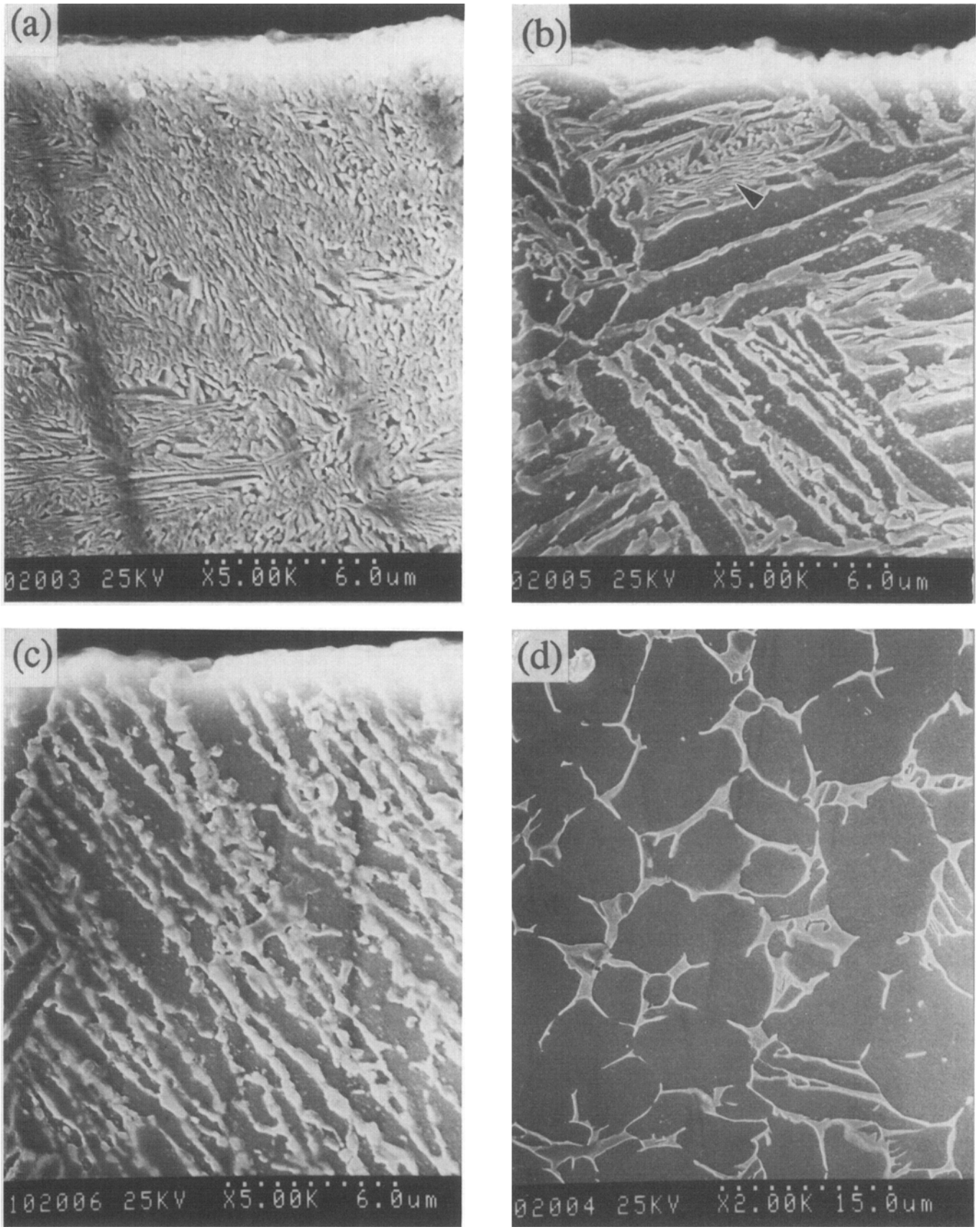

Fig. 3 SEM cross-sectional micrograph near the surface of (a) A2, (b) A4, (c) A8 specimens brazed at 960 °C for 2, 4, and 8 h, respectively, and (d) inner substrate

Figures 3(a), (b), and (c) show the SEM microstructure near the surface of the brazed materials after 2, 4, and 8 h; the light contrast feature is now the β phase and the dark contrast feature is the α phase. The fine and featureless zone A in Fig. 2(a) can be revealed in Fig. 3(a), which consists of fine lamellar α and β structure. After brazing for 4 h, some fine lamellar structure still exists in Fig. 3(b) (indicated by arrow), indicating probably some alloying element inhomogeneity. Figure 3(d) shows the equiaxed α plus intergranular β structure of Ti-6Al-4V substrate (i.e., zone C in Fig. 2). X-ray diffraction analyses of the vacuum-melted filler metal without brazing (A0 specimen) and the brazed materials near the surface after brazing heat treatment for 2, 4, and 8 h are shown in Fig. 4. The filler metal contains Ti_2Cu and Ti_2Ni phases in addition to α titanium (Fig. 4a). After brazing for 2 h, the surface of the brazed metal contains β titanium phase and some Ti_2Cu phase but nil Ti_2Ni, and minute Ti_2Cu phase may still exist in the brazed metal after brazing and diffusing for 8 h. Considering that the nickel content in Ti-21Ni-14Cu filler metal is higher than the copper content, the result might suggest that nickel diffuses faster than copper in the brazed titanium alloy, and this point is supported below. After diffusing for 8 h, preferential growth of α titanium of (102) plane at the expense of (101) plane can be observed in Fig. 4(d).

Transmission electron micrography near the surface of brazed Ti-21Ni-14Cu on Ti-6Al-4V substrate for 8 h is shown in Fig. 5, where α laths are separated by thin strip of β phase, similar to the counterpart SEM micrograph in Fig. 3(c). At the α/β interfaces, very occasional Ti_2Cu intermetallic phase was identified, confirming the XRD result in Fig. 4(d). Because copper is a β-stabilizing element, it partitions to the β phase from which coherent Ti_2Cu phase (η phase) grows at α-β interfaces. The η interface interphase has a crystallographic relation of $[110]_\eta//[111]_\beta$ and $(002)_\eta//(110)_\beta$ with the β phase. This

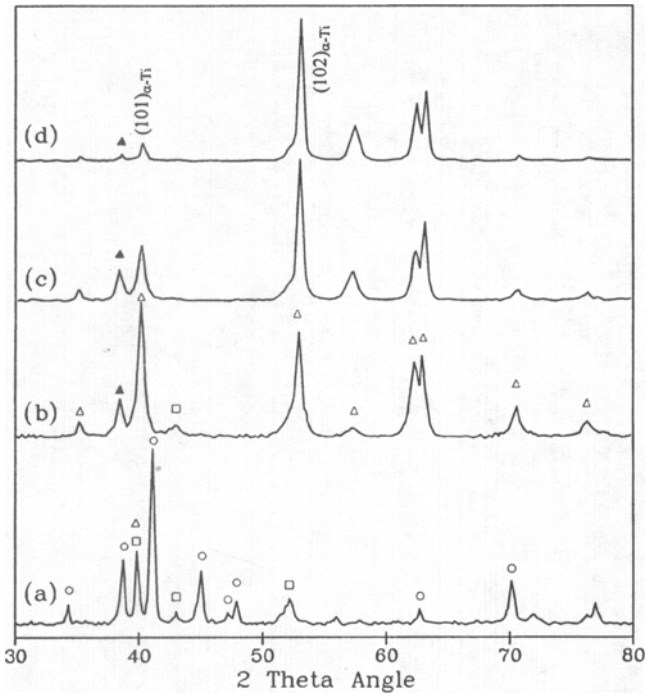

Fig. 4 XRD analyses on the surface of (a) A0, (b) A2, (c) A4, and (d) A8 specimens brazed at 960 °C for 0, 2, 4, and 8 h, respectively: open triangle, α Ti; filled triangle, β Ti; open circle, Ti_2Ni; open square, Ti_2Cu

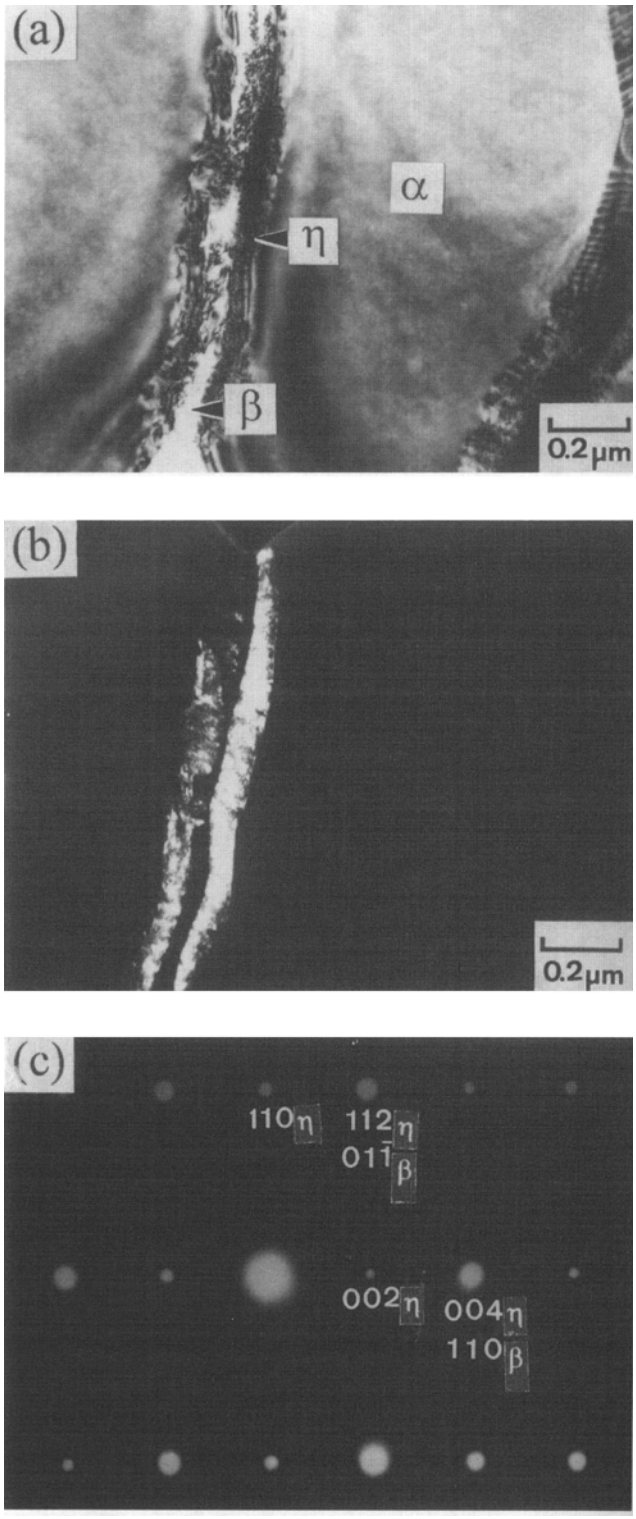

Fig. 5 TEM micrograph of A8 specimen showing (a) bright field image, (b) dark field image from Ti_2Cu (η) interphase, and (c) $[111]_\beta$ and $[110]_\eta$ zone diffraction pattern

phenomenon is similar to the precipitation of Ti_2Ni at α-β interface as suggested in Ref 8.

Figures 6(a) and (b) show the EDX chemical concentrations of copper and nickel atoms, respectively, measured from the surface and along the depth of the specimen brazed at 960 °C for 2, 4, and 8 h. As indicated in this figure, the concentration of copper and nickel was lowered to less than 3 to 4 wt% near the surface of specimen after brazing Ti-21Ni-14Cu on T-6Al-4V substrate at 960 °C for 8 h. The SEM cross-sectional micrograph and the corresponding distribution of copper and nickel atoms in the specimen brazed for 2 h is exhibited in Fig. 7. Figures 7(b) and (c) show the elemental distribution in zone B and in zone C near the zone B/zone C interface, respectively. Copper and nickel atoms are observed to partition to the β phase during the formation of Widmanstätten structure in zone B. The light contrast feature is the β phase, and the dark contrast feature is the α phase. It is indicated in Fig. 7(c) that the Ti-6Al-4V substrate at zone B/zone C interface contains more nickel than copper in β phase, indicating that inward diffusion of nickel along the β phase might be faster than that of copper. In the previous work, it was shown that nickel is a very effective element to lower the melting point of the titanium filler metal, but the element is also detrimental to the corrosion resistance of the titanium alloy. However, the implication from Fig. 7(c) and 4 is that the detrimental effect of nickel to corrosion resistance can be alleviated by a fast diffusion of the element during brazing to the substrate.

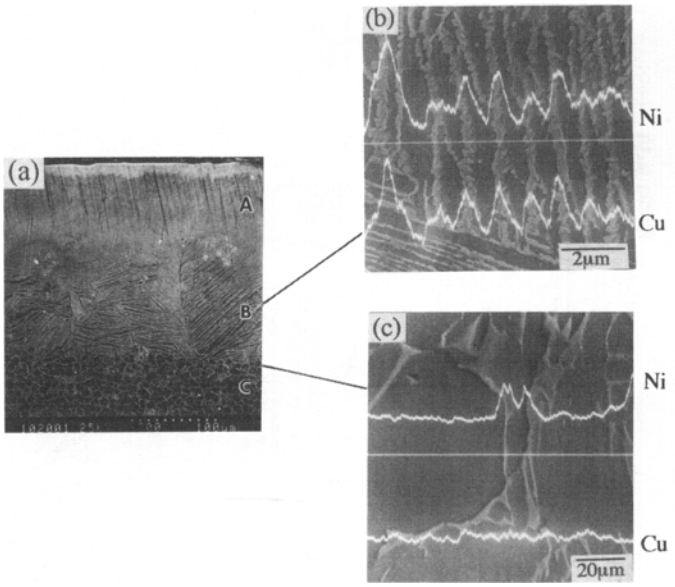

Fig. 7 Cross-sectional micrograph of A2 specimen showing (a) SEM microstructure, (b) line scan of copper and nickel in Widmanstätten structure of the brazing-affected zone, and (c) line scan of copper and nickel in equiaxed α plus intergranular β structure of Ti-6Al-4V substrate near the Widmanstätten/equiaxed zone interface

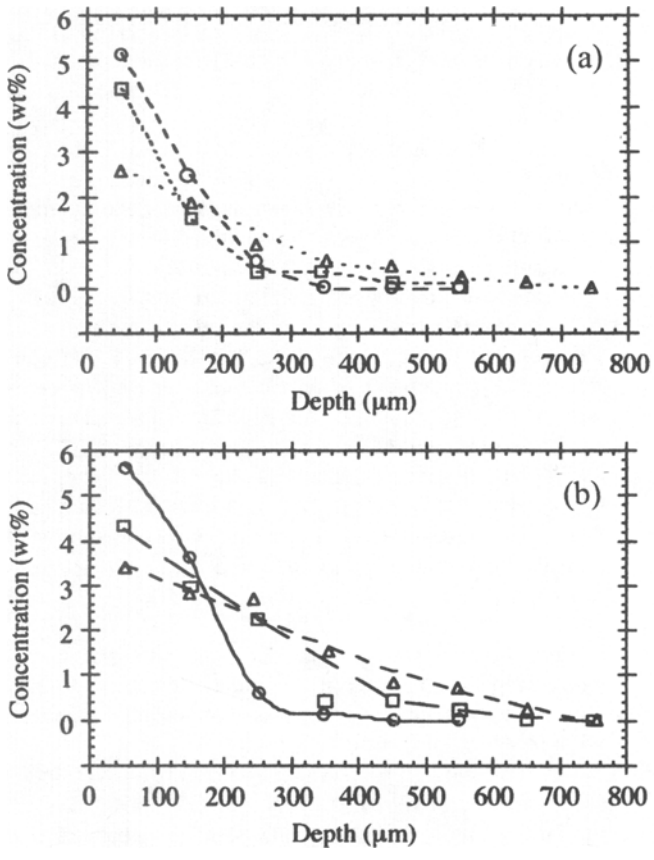

Fig. 6 EDX elemental distribution of (a) copper and (b) nickel as a function of depth from the surface of the brazed specimen: open circle, 2 h; open square, 4 h; open triangle, 8 h

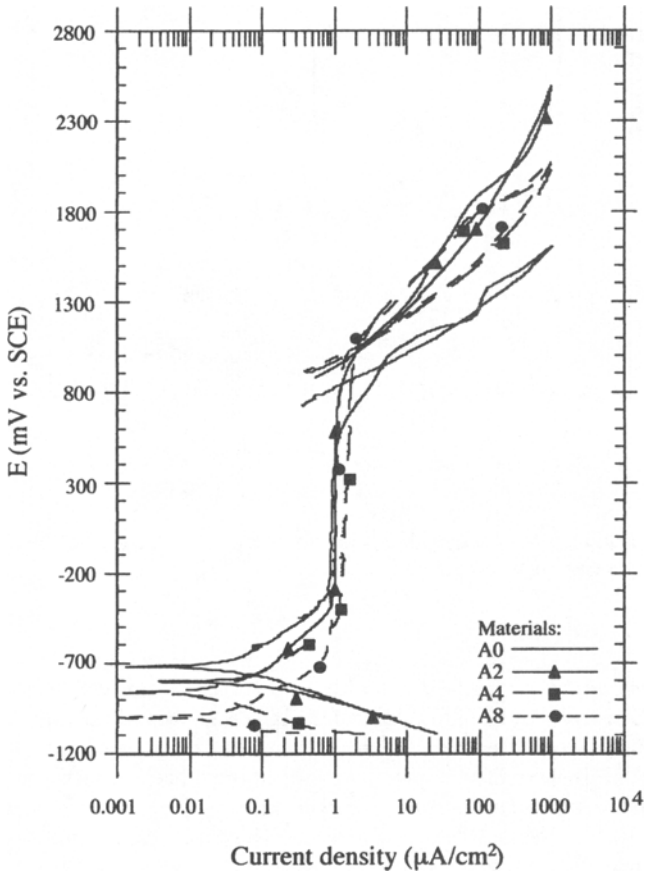

Fig. 8 Potentiodynamic polarization curves of A0, A2, A4, and A8 specimens in deaerated Hank's solution at 37 °C

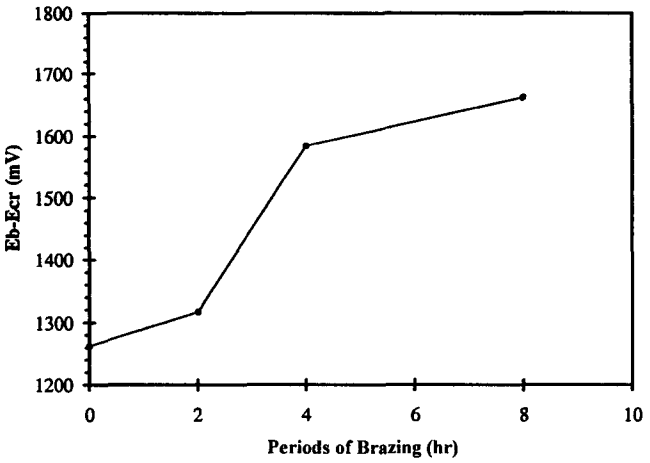

Fig. 9 Variation of passivation range as a function of the periods of brazing

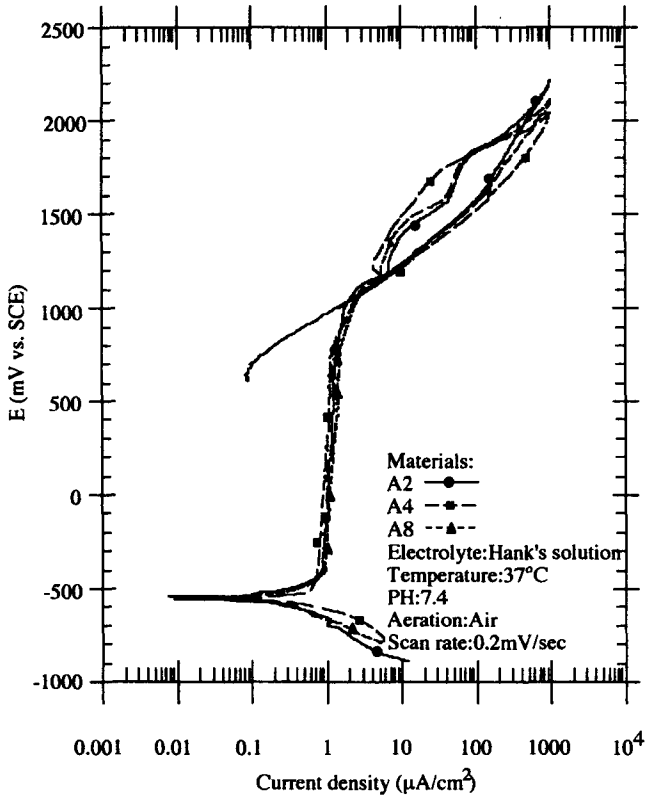

Fig. 10 Potentiodynamic polarization curves of A2, A4, and A8 specimens in aerated Hank's solution at 37 °C

The polarization curves of the vacuum-melted Ti-21Ni-14Cu filler metal, together with the brazed metals at 960 °C for 2, 4, and 8 h, tested in deaerated Hank's solution is shown in Fig. 8, and the electrochemical parameters are indicated in Table 1. In deaerated Hank's solution, all the brazed metals show broad passivation ranges (defined as E_b-E_{cr}) with more than 1300 mV versus saturated calomel electrode (SCE), and the current densities gradually increase after more than 909 mV versus SCE, which is higher than the equilibrium potential of oxygen generation (Ref 9). The data in Fig. 8 and Table 1 indicate that corrosion potential (E_{corr}), corrosion current density (i_{corr}), and critical potential for active-to-passive transition (E_{cr}) decrease while passivation range (E_b-E_{cr}) broadens with the period of brazing time, the reason being the corresponding decreases in intermetallic phase or copper and nickel atoms on the surface of the specimen as suggested in Fig. 4 and 6, respectively. The change of passivation range as a function of period of brazing is shown in Fig. 9.

The polarization curves of the specimens brazed at 960 °C for 2, 4, and 8 h and tested in oxygen-saturated Hank's solution are shown in Fig. 10, and the electrochemical parameters are indicated in Table 2. In oxygen-saturated Hank's solution, all the brazed metals show similar corrosion behaviors. The corrosion potentials for all the specimens lie within a narrow range between –525 and –547 mV versus SCE; the corrosion current densities are about 0.15 μA/cm^2; the passivation current densities are between 1.09 to 1.33 μA/cm^2; and the passivation ranges are above 1483 mV. Besides, the breakdown potentials are more than 1015 mV versus SCE, being higher than the equilibrium potential of oxygen generation (Ref 9). The results indicate that the existence of oxygen in Hank's solution promotes the corrosion potential and breakdown potential in the noble direction and reduces the range of E_{cr}-E_{corr}, meaning that the metals are readily passivated as the potential is polarized toward the oxidation direction.

4. Conclusion

- Although the Ti-21Ni-14Cu filler metal contains nil β phase, diffusion of copper and nickel from filler metal into the Ti-6Al-4V substrate at 960 °C for various periods has caused the Widmanstätten structure of lamellar α plus β to form in the brazing zone, while the structure of Ti-6Al-4V coarsens slightly. As the content of nickel and copper element has been lowered to less than 3 to 4 wt%, the chemical composition at brazed metal has changed from essentially a filler metal composition to the composition of Ti-6Al-4V substrate with only few remaining intermetallics.
- After brazing at 960 °C for 2 h, the surface of the brazed metal contains some Ti_2Cu phase, but the Ti_2Ni phase diminishes. The content of intermetallic phase decreases with brazing time, but minute Ti_2Cu phase may still exist in the brazed metal after brazing and diffusing for 8 h. The Ti_2Ni phase diminishes because nickel diffuses faster than copper along the β phase in Widmanstätten α plus β phase.
- The η interface interphase existing between α plus β phase appears to nucleate from the β phase, and it maintains a crystallographic relation of $[110]_\eta//[111]_\beta$ and $(002)_\eta//(110)_\beta$ with the β phase.
- In deaerated Hank's solution, corrosion potential, corrosion current density, and critical potential for active-to-passive transition decrease while passivation range broadens with the period of brazing time.
- In oxygen-saturated Hank's solution, all the brazed metals show similar corrosion behaviors. The existence of oxygen in Hank's solution promotes the corrosion potential and breakdown potential in the noble direction and reduces the range of E_{cr}-E_{corr}, meaning that the metals readily passivated as the potential is polarized in the oxidation direction.

Table 1 Parameters from the potentiodynamic polarization curves of A0, A2, A4, and A8 specimens in deaerated Hank's physiological solution at 37 °C

Materials	E_{corr}	i_{corr}	E_{cr}	i_{cr}	i_p	E_b	E_{pp}	E_b-E_{cr}	E_b-E_{pp}
A0	–720	0.049	–337	0.76	1.03	926	848	1263	78
A2	–776	0.089	–408	0.97	1.04	909	934	1317	...
A4	–899	0.023	–498	1.21	1.57	1086	1003	1584	83
A8	–1029	0.020	–710	0.84	1.02	953	982	1662	...

Current density: μA/cm^2, potential: mV versus SCE. E_{corr}: corrosion potential; i_{corr}: corrosion current density; E_{cr}: critical potential for active-to-passive transition; i_{cr}: critical current density for active-to-passive transition; i_p: passive current density; E_b: breakdown potential; E_{pp}: pit protection potential

Table 2 Parameters from the potentiodynamic polarization curves of A2, A4, and A8 specimens in aerated Hank's physiological solution at 37 °C

Materials	E_{corr}	i_{corr}	E_{cr}	i_{cr}	i_p	E_b	E_{pp}	E_b-E_{cr}	E_b-E_{pp}
A2	–525	0.16	–468	0.91	1.20	1015	990	1483	25
A4	–547	0.15	–522	0.78	1.09	1059	967	1581	92
A8	–534	0.15	–493	0.85	1.33	1031	994	1524	37

Current density: μA/cm^2, potential: mV versus SCE. E_{corr}: corrosion potential; i_{corr}: corrosion current density; E_{cr}: critical potential for active-to-passive transition; i_{cr}: critical current density for active-to-passive transition; i_p: passive current density; E_b: breakdown potential; E_{pp}: pit protection potential

References

1. D.G. Howden and R.W. Monroe, Suitable Alloys for Brazing Titanium Heat Exchangers, *Weld J.*, Vol 51 (No. 1), 1972, p 31-36
2. S.W. Lan, Laminated Brazing Filler Metals for Titanium Assemblies, *Weld. J.*, Vol 61 (No. 10), 1982, p 23-28
3. R.R. Well, Low Temperature Large-Area Brazing of Damage Tolerant Titanium Structures, *Weld. Res. Suppl.*, Vol 54 (No. 10), 1975, p 348-356
4. T. Onzawa, A. Suzumura, and M.W. Ko, Brazing of Titanium Using Low-Melting-Point Ti-Based Filler Metals, *Weld. Res. Suppl.*, Vol 69 (No. 12), 1990, p 462-467
5. E. Chang and C.H. Chen, Low-Melting-Point Titanium-Base Alloys—Part 1: Characteristics of Two-, Three- and Four-Component Filler Metals, *J. Mater. Eng. Perform.*, Vol 6 (No. 6), 1997, p 792-796
6. I. Tuah-Poku, M. Dollar, and T.B. Massalski, A Study of the Transient Liquid Phase Bonding Process Applied to a Ag/Cu/Ag Sandwich Joint, *Metall. Trans. A*, Vol 19 (No. 3), 1988, p 675-686
7. S.R. Seagle and L.J. Bartlo, Physical Metallurgy and Metallography of Titanium Alloys, *Titanium and Titanium Alloys Source Book*, M.J. Donachie, Jr., Ed., American Society for Metals, 1982, p 23-32
8. C.G. Rhodes, A.K. Ghosh, and R.A. Spurling, Ti-6Al-4V-2Ni as a Matrix Material for a SiC-Reinforced Composite, *Metall. Trans. A*, Vol 18 (No. 12), 1987, p 2151-2156
9. M. Pourbaix, *Atlas of Electrochemical Equilibria in Aqueous Solutions*, Pergamon Press, 1966